electronics

MDPI

Article

Takagi–Sugeno Observer Design for Remaining Useful Life Estimation of Li-Ion Battery System Under Faults

Norbert Kukurowski *, Marcin Pazera * and Marcin Witczak *

Institute of Control and Computation Engineering, University of Zielona Góra, ul. Szafrana 2, 65-516 Zielona Góra, Poland

* Correspondence: n.kukurowski@issi.uz.zgora.pl (N.K.); m.pazera@issi.uz.zgora.pl (M.P.); m.witczak@issi.uz.zgora.pl (M.W.)

Received: 25 August 2020; Accepted: 18 September 2020; Published: 20 September 2020

Abstract: Among the existing estimation schemes of a battery state of charge, most deal with an assumption that the faults will never occur in the system. Nevertheless, faults may have a crucial impact on the state of charge estimation accuracy. The paper proposes a novel observer design to estimate the state of charge and the remaining useful life of a Li-ion battery system under voltage and current measurement faults. The approach starts with converting the battery system into the descriptor Takagi–Sugeno form, where the state includes the original states along with the voltage and current measurement faults. Moreover, external disturbances are bounded by an ellipsoid based on the so-called Quadratic Boundedness approach, which ensures the system stability. The second-order Resistor-Capacitor equivalent circuit model is considered to verify the performance and correctness of the proposed observer. Subsequently, a real battery model is designed with experimental data of the Li-ion 18650 battery delivered from the NASA benchmark. Another experiment deals with an automated guided vehicle fed with a battery of which the remaining useful life is estimated. Finally, the results are compared with another estimation scheme based on the same benchmark.

Keywords: remaining useful life; Takagi–Sugeno fuzzy system; voltage and current measurement faults; observer design

1. Introduction

Nowadays, industrial companies are permanently increasing their productivity due to Industry 4.0. Consequently, a number of sensors and actuators have risen as well as intelligent warehouses by using Automated Guided Vehicles (AGVs). It is obvious that those vehicles mostly use battery systems, which need to be always recharged. Moreover, batteries sometimes should be replaced by fresh ones when their State Of Health (SOH) is low. Otherwise, the AGVs might stop in the middle of a task and consequently might breakdown the whole production cycle. This is why the Remaining Useful Life (RUL) estimation of a battery system is especially attractive.

In the recent literature, there are a lot of schemes that propose a State of Charge (SOC) estimation along with the assumption that the system is not occupied by any faults [1–3]. However, if these faults occur in the system, it will have a significant impact on the SOC estimation quality. There are, of course, schemes that deal with RUL estimation, for example, in [4] a data-driven hybrid RUL method for a real satellite Li-ion battery using an autoregressive model and a particle filter. Moreover, a satellite Li-ion battery RUL estimation was also presented in [5], where a Kalman Filter (KF) and relevance vector machine were used. Wu et al. [6], presented an online RUL estimation method for a Li-ion battery based on importance sampling and neural networks. However, Li et al. [7], described an RUL estimation

method for a Li-ion battery of an electric vehicle based on a support vector machine algorithm. A RUL prediction was made, as described in [8], which was based on a backward smoothing square root cubature KF. Moreover, a multiscale hybrid KF was used for the SOC estimation. Liu et al. [9] proposed a predicting method for RUL of Li-ion battery based on the framework of improved particle learning. Zhao et al. [10] presented a hybrid method for RUL estimation of a Li-ion battery along with a capacity regeneration. On the other hand, Guha et al. [11] proposed an electrochemical impedance spectrum and an RUL online estimation for a Li-ion battery. This method was based on a fractional-order equivalent circuit model. Yang et al. [12], described a prediction method based on an extreme learning machine for an RUL estimation of a Li-ion battery. Zhang et al. [13] presented a Li-ion battery online RUL estimation, which is based on thermal dynamics. Zhou et al. [14] proposed a Li-ion cells RUL estimation based on a nearest neighbor regression with a differential evolution optimization. Wei et al. [15] described a SOH diagnosis and RUL prediction for a Li-ion battery based on a support vector regression and particle filter. Wang et al. [16] presented an adaptive RUL estimation of a battery using a nonlinear degradation model. On the other side, in Ren et al. [17] a deep learning approach for a Li-ion battery RUL prediction was proposed. The proposed method was used with a real Li-ion battery data set from NASA. Ma et al. [18] described a prediction method for an RUL estimation based on a Gauss–Hermite particle filter for Li-ion batteries. Rauh et al. [19] introduced a nonlinear state observer based on extended KF for a finite-dimensional battery model. It should be also pointed out that such RUL estimation methods can form the base of a fault-tolerant control scheme for battery systems [20,21].

Finally, the above-listed approaches can be divided into two main groups:

- **Analytical**: they are based on the analytical RC models of the battery system. Most of these approaches inherit a common drawback that the underlying RC parameters are constant. Thus, it is beneficial to develop an approach that is able to settle the above problem assuming that RC parameters can vary in a given feasible set.
- **Data-driven**: they are based on soft computing techniques like fuzzy logic [22] and neural networks [23] or a combination of them. They also inherit a common drawback that a large amount of training and validation data is required. Indeed, the quality of such methods relies solely on the quality of data. Another drawback is that the models valid for a given battery system cannot be directly used for another one. This is caused by the fact that the models being using model merely the observed input–output relation while their parameters do not have any physical meaning.

To settle the above-mentioned difficulties it is proposed to use the Takagi–Sugeno model of the battery system [24–26]. Such models have proved to be very useful both for modeling and control of possibly time-varying and/or nonlinear systems [24]. Indeed, there is a large number of approaches that propose state and fault estimation techniques for T-S [27,28].

The novelty of the proposed RUL estimation scheme is that the system was transformed into Takagi–Sugeno form, where the state super-vector includes the original states as well as the voltage and current measurement faults. The appealing feature of the proposed approach is that it removes the problem of the so-called bounded current measurement fault rate of change as well as the one-step fault prediction, which is encountered in most fault estimation schemes. Subsequently, the so-called Quadratic Boundedness (QB) approach was considered to guarantee the system stability, where external disturbances are bounded by an ellipsoid. Moreover, the Takagi–Sugeno fuzzy battery system based on a second-order Resistor-Capacitor (RC) equivalent circuit model, was considered. Additionally, the proposed system is parameter-varying due to the fact that the parameters of the second-order RC model depend on the battery SOC.

The paper is organized as follows: Section 2 presents the battery system based on the second-order RC equivalent circuit model. Subsequently, the battery system was converted into the Takagi–Sugeno (T-S) fuzzy one. In Section 3, the robust observer design of a proposed T-S fuzzy system is described.

Additionally, the remaining useful life estimation scheme was considered for a battery system under voltage and current measurement faults. In Section 4, the response of the T-S fuzzy system was compared with an experimental data of the Li-ion battery. Consequently, results of the battery RUL estimation under faults were presented. Finally, the article was concluded in Section 5.

2. Battery System

The aim of the paper is to estimate an RUL of a battery system. Accordingly, the following second-order RC equivalent circuit model is considered:

$$\begin{cases} \dot{U}_1 = -\frac{U_1}{R_1 C_1} + \frac{I_b}{C_1}, \\ \dot{U}_2 = -\frac{U_2}{R_2 C_2} + \frac{Ib}{C_2}, \\ S\dot{O}C = \frac{I_b}{3600 C_b}, \end{cases} \tag{1}$$

where U_1,R_1,C_1 and U_2,R_2,C_2 are the voltage, resistance and capacity vectors of the first and second RC network, respectively. Furthermore, I_b indicates the battery current vector, where C_b signifies the nominal battery capacity, which is $C_b \approx 2Ah$ in this paper. Additionally, the graphical diagram of the second-order RC model is presented in Figure 1.

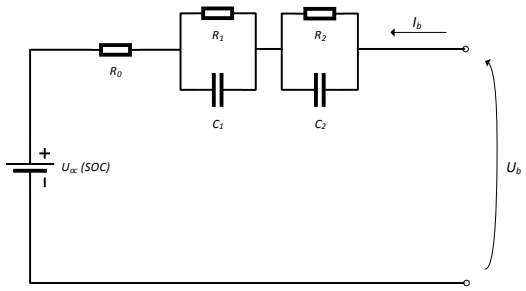

Figure 1. Second-order Resistor-Capacitor (RC) equivalent circuit model.

The following ninth-order polynomial method was used to characterize a nonlinearity between battery voltage and state of charge based on experimental data

$$\begin{aligned} U_{soc} = &-10.72 \cdot SOC^9 + 33.43 \cdot SOC^8 - 49.08 \cdot SOC^7 + 63.62 \cdot SOC^6 - 73.59 \cdot SOC^5 \\ &+ 51.05 \cdot SOC^4 - 15.21 \cdot SOC^3 + 0.1379 \cdot SOC^2 + 0.9428 \cdot SOC + 3.617, \end{aligned} \tag{2}$$

which is also illustrated in Figure 2.

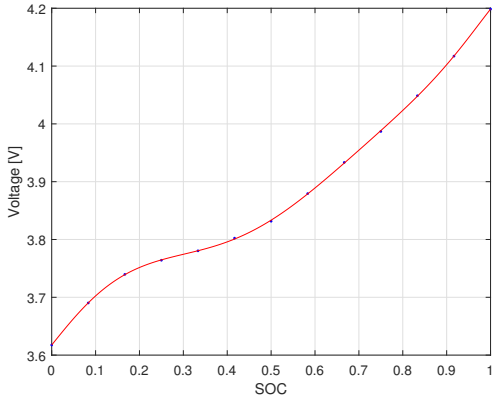

Figure 2. Nonlinear relationship of a battery state of charge and voltage.

Consequently, the battery voltage U_b can be obtained by

$$U_b = U_{soc} + U_1 + U_2 + R_0^i I_b, \tag{3}$$

where R_0 is the resistance vector. The proposed system is parameter varying based on the resistance as well as capacity parameters in Equations (3) and (4). These parameters depend on the battery SOC, as illustrated in Table 1. Using parameters contained in Table 1 along with the approach presented in [29], the system described by Equation (1) can be parameterized as follows:

$$\boldsymbol{A}^i = \begin{bmatrix} -\frac{1}{R_1^i C_1^i} & 0 & 0 \\ 0 & -\frac{1}{R_2^i C_2^i} & 0 \\ 0 & 0 & 0 \end{bmatrix}, \quad \boldsymbol{B}^i = \begin{bmatrix} \frac{1}{C_1^i} \\ \frac{1}{C_2^i} \\ \frac{1}{3600 C_b} \end{bmatrix}, \quad \boldsymbol{C} = \begin{bmatrix} 1 & 0 & 0 \\ 0 & 1 & 0 \end{bmatrix}, \tag{4}$$

where i corresponds to the ith row of Table 1. Note that there is a single cell only. While its parameters R_0, R_1, C_1, R_2, C_2 may vary in time. That is why they are divided into 13 representative values R_0^i, R_1^i, C_1^i, R_2^i, C_2^i while the current operating condition depends on SOC. Moreover, the above model is simplified, and hence, it does not take into account a possibly time-varying temperature [30]. In other words, the system is operating in a constant room temperature. Subsequently, the Gaussian membership functions $\mu_{i,k}$ were used to form the Takagi–Sugeno system, with means equal to the SOC values given in Table 1 and standard deviations equal to the distance between consecutive SOC values. As a result, the following models were obtained:

$$\boldsymbol{x}_{k+1} = \sum_{i=1}^{M} h_i\left(\boldsymbol{q}_k\right)\left[\boldsymbol{A}^i \boldsymbol{x}_k + \boldsymbol{B}^i \boldsymbol{I}_{b,k}\right], \tag{5}$$

$$\boldsymbol{y}_k = \boldsymbol{C}\boldsymbol{x}_k, \tag{6}$$

where $\boldsymbol{q}_k = SOC_k$. Note that matrices in Equation (4) simply form TS model Equation (5) and

$$h_i\left(\boldsymbol{q}_k\right) = \frac{\mu_{i,k}}{\sum_{j=1}^{M} \mu_{j,k}}. \tag{7}$$

Note that all matrices shaping the above model are described in Appendix A. Having the above model, it is possible to proceed to the SOC estimator design.

Table 1. Parameters of the second-order RC model.

SOC	$R_0[\Omega]$	$R_1[\Omega]$	$R_2[\Omega]$	$C_1[F]$	$C_2[F]$
0	0.18777	0.016782	0.10044	574.2	935.5
0.083	0.15643	0.019272	0.041271	492.44	2225.1
0.167	0.15797	0.018844	0.040802	494.31	2226
0.25	0.16243	0.018733	0.040952	487.87	2272.6
0.33	0.16355	0.018036	0.040065	512.41	2209.8
0.417	0.15656	0.018058	0.039243	519.19	2190.4
0.5	0.16255	0.01858	0.039791	498.86	2189.8
0.583	0.15325	0.018479	0.039945	498.46	2239.7
0.667	0.16402	0.018512	0.040019	489.93	2294.8
0.75	0.15714	0.019181	0.039949	500.61	2424.3
0.833	0.15489	0.019026	0.040046	502.43	2420
0.917	0.15324	0.019026	0.040046	502.43	2420
1	0.15996	0.016109	0.043569	593.18	2224.4

3. Observer Design

Firstly, using (5) and (6), let us formulate a discrete-time Takagi–Sugeno fuzzy system, which can be affected by faults and disturbances:

$$\boldsymbol{x}_{k+1} = \sum_{i=1}^{M} h_i\left(\boldsymbol{q}_k\right)\left[\boldsymbol{A}^i\boldsymbol{x}_k + \boldsymbol{B}^i\boldsymbol{I}_{b,k} + \boldsymbol{B}^i_f\bar{\boldsymbol{f}}_{a,k}\right] + \boldsymbol{W}_1\boldsymbol{w}_{1,k}, \tag{8}$$

$$\boldsymbol{y}_k = \boldsymbol{C}\boldsymbol{x}_k + \boldsymbol{C}_f\boldsymbol{f}_{s,k} + \boldsymbol{W}_2\boldsymbol{w}_{2,k}, \tag{9}$$

with

$$h_i(\boldsymbol{q}_k) \geq 0, \qquad \forall i = 1,\ldots,M, \qquad \sum_{i=1}^{M} h_i(\boldsymbol{q}_k) = 1, \tag{10}$$

where k indicates a discrete time as well as $\boldsymbol{x}_k = \begin{bmatrix} U_1 & U_2 & SOC \end{bmatrix}^T \in \mathbb{X} \subset \mathbb{R}^n$, $\boldsymbol{I}_{b,k} \in \mathbb{R}^r$ and $\boldsymbol{y}_k = \begin{bmatrix} U_1 & U_2 \end{bmatrix}^T \in \mathbb{R}^m$ signify state, input and output vectors, respectively. Subsequently, $\boldsymbol{f}_{s,k} \in \mathbb{F}_s \subset \mathbb{R}^{n_s}$ and $\bar{\boldsymbol{f}}_{a,k} \in \mathbb{F}_a \subset \mathbb{R}^{n_a}$ describe the voltage (e.g., a broken wire) and current measurement fault vectors, while n_s and n_a indicate the number of voltage and current measurement faults, respectively. Moreover, the voltage measurement fault distribution matrix is denoted by $\boldsymbol{C}_f$, while $\text{rank}(\boldsymbol{C}_f) = n_s$ and $\text{rank}(\boldsymbol{B}_f(\boldsymbol{q}_k)) = n_a$. Additionally, the inequality $n_a + n_s \leq m$ is satisfied, which means that there is no possibility that the number of reconstructed faults is greater than the number of measured outputs. Furthermore, the disturbance distribution matrices are indicated by $\boldsymbol{W}_1$ and $\boldsymbol{W}_2$, where exogenous disturbance vectors for measurement and process uncertainties are denoted by $\boldsymbol{w}_{1,k}$ and $\boldsymbol{w}_{2,k}$, respectively. Additionally, let us use the following notation throughout the paper $\boldsymbol{X}^i = \sum_{i=1}^{M} h_i\left(\boldsymbol{q}_k\right)\boldsymbol{X}^i$. Let us first transform the state Equation (8) into an equivalent form

$$\boldsymbol{x}_{k+1} = \sum_{i=1}^{M} h_i^i\left[\boldsymbol{A}^i\boldsymbol{x}_k + \boldsymbol{B}^i\boldsymbol{I}_{b,k}\right] + \boldsymbol{B}_f\boldsymbol{f}_{a,k} + \boldsymbol{W}_1\boldsymbol{w}_{1,k}, \tag{11}$$

where $\boldsymbol{B}_f$ indicates an auxiliary matrix, which satisfy $\text{rank}(\boldsymbol{B}_f) = n_a$ as well as $\boldsymbol{f}_{a,k}$ states for an auxiliary current measurement fault vector. Consequently, by comparing Equations (8) and (11), it can be easily seen that

$$\boldsymbol{B}_f(\boldsymbol{q}_k)\bar{\boldsymbol{f}}_{a,k} = \boldsymbol{B}_f\boldsymbol{f}_{a,k}. \tag{12}$$

Hence, the following original fault vector can be defined

$$\bar{\boldsymbol{f}}_{a,k} = (\boldsymbol{B}_f(\boldsymbol{q}_k))^{\dagger}\boldsymbol{B}_f\boldsymbol{f}_{a,k}. \tag{13}$$

where † indicates the pseudo inverse operator. Furthermore, let us describe a novel observer able for estimating $\boldsymbol{x}_k$, $\boldsymbol{f}_{a,k}$ and $\boldsymbol{f}_{s,k}$ simultaneously, which is the purpose of further considerations. Additionally, it can be observed that $\boldsymbol{B}_f = \frac{1}{M}\sum_{i=1}^{M}\boldsymbol{B}_f^i$ as well as $\text{rank}(\boldsymbol{B}_f) = n_a$, which means that the selected $\boldsymbol{B}_f$ is not critical. The proposed scheme begins with converting Equations (9)–(11) into an equivalent, descriptor-like form, where the state variable is given as

$$\bar{\boldsymbol{x}}_k = \begin{bmatrix}\boldsymbol{x}_k^T & \boldsymbol{f}_{a,k-1}^T & \boldsymbol{f}_{s,k}^T\end{bmatrix}^T. \tag{14}$$

Based on Equation (14), the system Equations (9)–(11) can be described as follow:

$$\boldsymbol{E}\bar{\boldsymbol{x}}_{k+1} = \bar{\boldsymbol{A}}^i\bar{\boldsymbol{x}}_k + \bar{\boldsymbol{B}}^i\boldsymbol{I}_{b,k} + \bar{\boldsymbol{W}}_1\bar{\boldsymbol{w}}_k, \tag{15}$$

$$\boldsymbol{y}_k = \bar{\boldsymbol{C}}\boldsymbol{x}_k + \bar{\boldsymbol{W}}_2\bar{\boldsymbol{w}}_k, \tag{16}$$

where:

$$\boldsymbol{E} = \begin{bmatrix}\boldsymbol{I}_n & -\boldsymbol{B}_f & \boldsymbol{0}\\ \boldsymbol{0} & \boldsymbol{0} & \boldsymbol{0}\\ \boldsymbol{0} & \boldsymbol{0} & \boldsymbol{0}\end{bmatrix}, \quad \bar{\boldsymbol{A}}^i = \begin{bmatrix}\boldsymbol{A}^i & \boldsymbol{0} & \boldsymbol{0}\\ \boldsymbol{0} & \boldsymbol{0} & \boldsymbol{0}\\ \boldsymbol{0} & \boldsymbol{0} & \boldsymbol{0}\end{bmatrix}, \quad \bar{\boldsymbol{B}}^i = \begin{bmatrix}\boldsymbol{B}^i\\ \boldsymbol{0}\\ \boldsymbol{0}\end{bmatrix},$$

$$\bar{\boldsymbol{W}}_1 = \begin{bmatrix}\boldsymbol{W}_1 & \boldsymbol{0}\\ \boldsymbol{0} & \boldsymbol{0}\\ \boldsymbol{0} & \boldsymbol{0}\end{bmatrix}, \quad \bar{\boldsymbol{W}}_2 = \begin{bmatrix}\boldsymbol{0} & \boldsymbol{W}_2\end{bmatrix}, \quad \bar{\boldsymbol{w}}_k = \begin{bmatrix}\boldsymbol{w}_{1,k}^T & \boldsymbol{w}_{2,k}^T\end{bmatrix}^T, \quad \bar{\boldsymbol{C}} = \begin{bmatrix}\boldsymbol{C}^T\\ \boldsymbol{0}\\ \boldsymbol{C}_f^T\end{bmatrix}^T.$$

That means, the state super-vector $\bar{\boldsymbol{x}}_k$ includes the original state of the system as well as voltage and current measurement faults. Consequently, let us propose the following observer:

$$\boldsymbol{z}_{k+1} = \boldsymbol{H}^i\boldsymbol{z}_k + \boldsymbol{M}^i\boldsymbol{I}_{b,k} + \boldsymbol{F}^i\boldsymbol{y}_k, \tag{17}$$

$$\hat{\bar{\boldsymbol{x}}}_k = \boldsymbol{z}_k + \mathcal{T}_2\boldsymbol{y}_k, \tag{18}$$

where $\hat{\bar{\boldsymbol{x}}}_k \in \mathbb{R}^{n+na+ns}$ indicates the estimate of $\bar{\boldsymbol{x}}_k$ as well as $\boldsymbol{z}_k \in \mathbb{R}^{n+na+ns}$ denotes the internal state of the estimator. Note that the typical assumption in the recent literature respecting a bounded rate of change of occurred faults was removed by proposing this novel scheme.

Accordingly, let it be assumed that there are existing matrices $\mathcal{T}_1$ and $\mathcal{T}_2$ such that

$$\mathcal{T}_1\boldsymbol{E} + \mathcal{T}_2\bar{\boldsymbol{C}} = \boldsymbol{I}, \tag{19}$$

or in simpler form

$$\begin{bmatrix}\mathcal{T}_1 & \mathcal{T}_2\end{bmatrix}\begin{bmatrix}\boldsymbol{E}\\ \bar{\boldsymbol{C}}\end{bmatrix} = \boldsymbol{I}, \tag{20}$$

which gives Equations (17) and (18) the following design condition

$$\operatorname{rank}\left(\begin{bmatrix} \boldsymbol{E} \\ \bar{\boldsymbol{C}} \end{bmatrix}\right) = n + n_a + n_s. \tag{21}$$

Based on the above assumption and Equation (18), the state estimation error is given as

$$\boldsymbol{e}_k = \bar{\boldsymbol{x}}_k - \hat{\bar{\boldsymbol{x}}}_k = \bar{\boldsymbol{x}}_k - \boldsymbol{z}_k - \mathcal{T}_2 \boldsymbol{y}_k = \left(\boldsymbol{I} - \mathcal{T}_2 \bar{\boldsymbol{C}}\right) \bar{\boldsymbol{x}}_k - \boldsymbol{z}_k - \mathcal{T}_2 \bar{\boldsymbol{W}}_2 \bar{\boldsymbol{w}}_k, \tag{22}$$

which, according to Equation (19), is reduced to

$$\boldsymbol{e}_k = \mathcal{T}_1 \boldsymbol{E} \bar{\boldsymbol{x}}_k - \boldsymbol{z}_k - \mathcal{T}_2 \bar{\boldsymbol{W}}_2 \bar{\boldsymbol{w}}_k. \tag{23}$$

Additionally, the state estimation error dynamics can be defined by substituting Equations (15)–(17)

$$\begin{aligned} \boldsymbol{e}_{k+1} &= \mathcal{T}_1 \boldsymbol{E} \bar{\boldsymbol{x}}_{k+1} - \boldsymbol{z}_{k+1} - \mathcal{T}_2 \bar{\boldsymbol{W}}_2 \bar{\boldsymbol{w}}_{k+1} = \mathcal{T}_1 \bar{\boldsymbol{A}}^i \bar{\boldsymbol{x}}_k + \mathcal{T}_1 \bar{\boldsymbol{B}}^i \boldsymbol{I}_{b,k} \\ &+ \mathcal{T}_1 \bar{\boldsymbol{W}}_1 \bar{\boldsymbol{w}}_k - \boldsymbol{H}^i \boldsymbol{z}_k - \boldsymbol{M}^i \boldsymbol{I}_{b,k} - \boldsymbol{F}^i \bar{\boldsymbol{C}} \bar{\boldsymbol{x}}_k - \boldsymbol{F}^i \bar{\boldsymbol{W}}_2 \bar{\boldsymbol{w}}_k - \mathcal{T}_2 \bar{\boldsymbol{W}}_2 \bar{\boldsymbol{w}}_{k+1} \\ &= \left(\mathcal{T}_1 \bar{\boldsymbol{A}}^i - \boldsymbol{F}^i \bar{\boldsymbol{C}} -^i \mathcal{T}_1 \boldsymbol{E}\right) \bar{\boldsymbol{x}}_k + \left(\mathcal{T}_1 \bar{\boldsymbol{B}}^i - \boldsymbol{M}^i\right) \boldsymbol{I}_{b,k} \\ &+ \boldsymbol{H}^i \boldsymbol{e}_k + \left(\mathcal{T}_1 \bar{\boldsymbol{W}}_1 - \boldsymbol{F}^i \bar{\boldsymbol{W}}_2 + \boldsymbol{H}^i \mathcal{T}_2 \bar{\boldsymbol{W}}_2\right) \bar{\boldsymbol{w}}_k - \mathcal{T}_2 \bar{\boldsymbol{W}}_2 \bar{\boldsymbol{w}}_{k+1}. \end{aligned} \tag{24}$$

Based on Equation (24), it is obvious that the following conditions should be considered:

$$\mathcal{T}_1 \bar{\boldsymbol{A}}^i - \boldsymbol{H}^i \mathcal{T}_1 \boldsymbol{E} - \boldsymbol{F}^i \bar{\boldsymbol{C}} = 0, \tag{25}$$

$$\mathcal{T}_1 \bar{\boldsymbol{B}}^i - \boldsymbol{M}^i = 0. \tag{26}$$

Accordingly, by satisfying above Equations (25) and (26), the term concerned $\bar{\boldsymbol{x}}_k$ is removed from Equation (24) as well as Equation (25) is from now independent of the system input vector $\boldsymbol{I}_{b,k}$. Moreover, substituting Equation (19) into Equation (25) provides

$$\mathcal{T}_1 \bar{\boldsymbol{A}}^i - \boldsymbol{H}^i \left(\boldsymbol{I} - \mathcal{T}_2 \bar{\boldsymbol{C}}\right) - \boldsymbol{F}^i \bar{\boldsymbol{C}} = 0, \tag{27}$$

or in simpler form

$$\boldsymbol{H}^i = \mathcal{T}_1 \bar{\boldsymbol{A}}^i - \left(\boldsymbol{F}^i - \boldsymbol{H}^i \mathcal{T}_2\right) \bar{\boldsymbol{C}}. \tag{28}$$

Consequently, by determining

$$\boldsymbol{K}^i = \boldsymbol{F}^i - \boldsymbol{H}^i \mathcal{T}_2, \tag{29}$$

Equation (28) is reduced to

$$\boldsymbol{H}^i = \mathcal{T}_1 \bar{\boldsymbol{A}}^i - \boldsymbol{K}^i \bar{\boldsymbol{C}}, \tag{30}$$

which modifies Equation (24) into

$$\begin{aligned} \boldsymbol{e}_{k+1} &= \boldsymbol{H}^i \boldsymbol{e}_k + \left(\mathcal{T}_1 \bar{\boldsymbol{W}}_1 - \boldsymbol{F}^i \bar{\boldsymbol{W}}_2 + \boldsymbol{H}^i \mathcal{T}_2 \bar{\boldsymbol{W}}_2\right) \bar{\boldsymbol{w}}_k - \mathcal{T}_2 \bar{\boldsymbol{W}}_2 \bar{\boldsymbol{w}}_{k+1} \\ &= \left(\mathcal{T}_1 \bar{\boldsymbol{A}}^i - \boldsymbol{K}^i \bar{\boldsymbol{C}}\right) \boldsymbol{e}_k + \mathcal{T}_1 \bar{\boldsymbol{W}}_1 \bar{\boldsymbol{w}}_k - \boldsymbol{K}^i \bar{\boldsymbol{W}}_2 \bar{\boldsymbol{w}}_k - \boldsymbol{H}^i \mathcal{T}_2 \bar{\boldsymbol{W}}_2 \bar{\boldsymbol{w}}_k \\ &+ \boldsymbol{H}^i \mathcal{T}_2 \bar{\boldsymbol{W}}_2 \bar{\boldsymbol{w}}_k - \mathcal{T}_2 \bar{\boldsymbol{W}}_2 \bar{\boldsymbol{w}}_{k+1} = \left(\mathcal{T}_1 \bar{\boldsymbol{A}}^i - \boldsymbol{K}^i \bar{\boldsymbol{C}}\right) \boldsymbol{e}_k \\ &+ \mathcal{T}_1 \bar{\boldsymbol{W}}_1 \bar{\boldsymbol{w}}_k - \boldsymbol{K}^i \bar{\boldsymbol{W}}_2 \bar{\boldsymbol{w}}_k - \mathcal{T}_2 \bar{\boldsymbol{W}}_2 \bar{\boldsymbol{w}}_{k+1}. \end{aligned} \tag{31}$$

Furthermore, let the state super-vector be defined as follows

$$\tilde{\boldsymbol{w}}_k = \begin{bmatrix} \bar{\boldsymbol{w}}_k \\ \bar{\boldsymbol{w}}_{k+1} \end{bmatrix}, \tag{32}$$

and consequently, Equation (31) can be replaced by its simpler form

$$\boldsymbol{e}_{k+1} = \boldsymbol{X}^i \boldsymbol{e}_k + \boldsymbol{Z}^i \tilde{\boldsymbol{w}}_k, \tag{33}$$

with:

$$\boldsymbol{X}^i = \tilde{\boldsymbol{A}}^i - \boldsymbol{K}^i \bar{\boldsymbol{C}}, \qquad \boldsymbol{Z}^i = \tilde{\boldsymbol{W}}_1 - \boldsymbol{K}^i \tilde{\boldsymbol{W}}_2,$$

where:

$$\tilde{\boldsymbol{W}}_1^i = \begin{bmatrix} \mathcal{T}_1 \bar{\boldsymbol{W}}_1 & -\mathcal{T}_2 \bar{\boldsymbol{W}}_2 \end{bmatrix}, \quad \tilde{\boldsymbol{W}}_2 = \begin{bmatrix} \bar{\boldsymbol{W}}_2 & \boldsymbol{0} \end{bmatrix}, \quad \tilde{\boldsymbol{A}}^i = \mathcal{T}_1 \bar{\boldsymbol{A}}^i.$$

Taking into account the above considerations, let us recall the following Lemma [31]:

Lemma 1. *The following statements are equivalent:*

1. *There exist* $\boldsymbol{X} \succ 0$ *and* $\boldsymbol{W} \succ 0$ *such that*

$$\boldsymbol{V}^{i,T} \boldsymbol{X} \boldsymbol{V}^i - \boldsymbol{W} \prec 0, \tag{34}$$

where $\boldsymbol{X} \prec 0$ *means that matrix* $\boldsymbol{X}$ *is negative definite whilst* $\boldsymbol{X} \succ$ *means that matrix* $\boldsymbol{X}$ *is positive definite.*

2. *There exist* $\boldsymbol{X} \succ 0$, $\boldsymbol{W} \succ 0$ *and* $\boldsymbol{U}$ *such that*

$$\begin{bmatrix} -\boldsymbol{W} & \boldsymbol{V}^{i,T} \boldsymbol{U}^T \\ \boldsymbol{U} \boldsymbol{V}^i & \boldsymbol{X} - \boldsymbol{U} - \boldsymbol{U}^T \end{bmatrix} \prec 0. \tag{35}$$

Let the Lyapunov function be described as follows

$$V_k = \boldsymbol{e}_k^T \boldsymbol{R} \boldsymbol{e}_k, \tag{36}$$

with $\boldsymbol{R} \succ 0$. The convergence of the proposed observer is to be determined with the so-called Quadratic Boundedness (QB) approach [32]. This technique can be perceived as an extension of the usual Lyapunov approach towards the systems with external bounded disturbances. The usefulness of the QB approach was proven in many papers while in [33] it was proven that the standard $\mathcal{H}_\infty$ framework can be perceived as a special case of QB. To use the QB approach, it is necessary to assume that $\tilde{\boldsymbol{w}}_k$ is bounded by the following ellipsoid:

$$\mathbb{E}_w = \{\tilde{\boldsymbol{w}}_k : \ \tilde{\boldsymbol{w}}_k^T \boldsymbol{Q}_w \tilde{\boldsymbol{w}}_k \leq 1\}, \tag{37}$$

with $\boldsymbol{Q}_w \succ 0$. Based upon the above assumptions, let us recall the following definition:

Definition 1. *The system Equation* (33) *is strictly quadratically bounded for all* $\tilde{\boldsymbol{w}}_k \in \mathbb{E}_w$, $k \geq 0$, *if* $V_k > 1 \implies V_{k+1} - V_k < 0$ *for any* $\tilde{\boldsymbol{w}}_k \in \mathbb{E}_w$.

As it was described in [32,33], the stability condition is associated with

$$V_{k+1} - (1-\alpha)\, V_k - \alpha \tilde{\boldsymbol{w}}_k^T \boldsymbol{Q}_w \tilde{\boldsymbol{w}}_k < 0, \tag{38}$$

with $0 < \alpha < 1$. Taking into account the above deliberations, the following theorem is stated:

Theorem 1. *The observer-based system Equation (33) is strictly quadratically bounded for all $\tilde{\boldsymbol{w}}_k \in \mathbb{E}_w$ if there exist matrices $\boldsymbol{R} \succ 0$, $\boldsymbol{U}$, $\tilde{\boldsymbol{N}}$ as well as $\alpha \in (0,1)$ such that the following holds:*

$$\begin{bmatrix} \alpha\boldsymbol{R} - \boldsymbol{R} & \boldsymbol{0} & \tilde{\boldsymbol{A}}^{i,T}\boldsymbol{U}^T - \bar{\boldsymbol{C}}^T\tilde{\boldsymbol{N}}^{i,T} \\ \boldsymbol{0} & -\alpha\boldsymbol{Q}_w & \tilde{\boldsymbol{W}}_1^T\boldsymbol{U}^T - \tilde{\boldsymbol{W}}_2^T\tilde{\boldsymbol{N}}^{i,T} \\ \boldsymbol{U}\tilde{\boldsymbol{A}}^i - \tilde{\boldsymbol{N}}^i\bar{\boldsymbol{C}} & \boldsymbol{U}\tilde{\boldsymbol{W}}_1 - \tilde{\boldsymbol{N}}^i\tilde{\boldsymbol{W}}_2 & \boldsymbol{R} - \boldsymbol{U} - \boldsymbol{U}^T \end{bmatrix} \prec 0. \tag{39}$$

Proof. The stability condition (38) leads to

$$\boldsymbol{e}_{k+1}^T\boldsymbol{R}\boldsymbol{e}_k - \boldsymbol{e}_k^T\boldsymbol{R}\boldsymbol{e}_k + \alpha\boldsymbol{e}_k^T\boldsymbol{R}\boldsymbol{e}_k - \alpha\tilde{\boldsymbol{w}}_k^T\boldsymbol{Q}_w\tilde{\boldsymbol{w}}_k < 0. \tag{40}$$

Using (33) it can be shown that (40) can be equivalently rewritten as

$$\begin{aligned} &\boldsymbol{e}_k^T\left(\boldsymbol{X}^{i,T}\boldsymbol{R}\boldsymbol{X}^i + \alpha\boldsymbol{R} - \boldsymbol{R}\right)\boldsymbol{e}_k + \boldsymbol{e}_k^T\left(\boldsymbol{X}^{i,T}\boldsymbol{R}\boldsymbol{Z}\right)\tilde{\boldsymbol{w}}_k + \tilde{\boldsymbol{w}}_k^T\left(\boldsymbol{Z}^T\boldsymbol{R}\boldsymbol{X}^i\right)\boldsymbol{e}_k \\ &+ \tilde{\boldsymbol{w}}_k^T\left(\boldsymbol{Z}^T\boldsymbol{R}\boldsymbol{Z} - \alpha\boldsymbol{Q}_w\right)\tilde{\boldsymbol{w}}_k \prec 0. \end{aligned} \tag{41}$$

By setting

$$\boldsymbol{v}_k = \begin{bmatrix} \boldsymbol{e}_k \\ \tilde{\boldsymbol{w}}_k \end{bmatrix}, \tag{42}$$

formula (41) can be rephrased into the following form

$$\boldsymbol{v}_k^T\begin{bmatrix} \boldsymbol{X}^{i,T}\boldsymbol{R}\boldsymbol{X} + \alpha\boldsymbol{R} - \boldsymbol{R} & \boldsymbol{X}^{i,T}\boldsymbol{R}\boldsymbol{Z} \\ \boldsymbol{Z}^T\boldsymbol{R}\boldsymbol{X}^i & \boldsymbol{Z}^T\boldsymbol{R}\boldsymbol{Z} - \alpha\boldsymbol{Q}_w \end{bmatrix}\boldsymbol{v}_k \prec 0, \tag{43}$$

or an alternative one

$$\begin{bmatrix} \boldsymbol{X}^{i,T} \\ \boldsymbol{Z}^T \end{bmatrix}\boldsymbol{R}\begin{bmatrix} \boldsymbol{X}^i & \boldsymbol{Z} \end{bmatrix} + \begin{bmatrix} \alpha\boldsymbol{R} - \boldsymbol{R} & \boldsymbol{0} \\ \boldsymbol{0} & -\alpha\boldsymbol{Q}_w \end{bmatrix} \prec 0. \tag{44}$$

then, applying Lemma (1) to (44) results in

$$\begin{bmatrix} \boldsymbol{R} + \alpha\boldsymbol{R} & \boldsymbol{0} & \boldsymbol{X}^{i,T}\boldsymbol{U}^T \\ \boldsymbol{0} & -\alpha\boldsymbol{Q}_w & \boldsymbol{Z}^T\boldsymbol{U}^T \\ \boldsymbol{U}\boldsymbol{X}^i & \boldsymbol{U}\boldsymbol{Z} & \boldsymbol{R} - \boldsymbol{U} - \boldsymbol{U}^T \end{bmatrix} \prec 0. \tag{45}$$

Finally, substituting

$$\boldsymbol{U}\boldsymbol{X}^i = \boldsymbol{U}\left(\tilde{\boldsymbol{A}}^i - \boldsymbol{K}^i\bar{\boldsymbol{C}}\right) = \boldsymbol{U}\tilde{\boldsymbol{A}}^i - \tilde{\boldsymbol{N}}^i\bar{\boldsymbol{C}}, \tag{46}$$

$$\boldsymbol{U}\boldsymbol{Z}^i = \boldsymbol{U}\left(\tilde{\boldsymbol{W}}_1 - \boldsymbol{K}^i\tilde{\boldsymbol{W}}_2\right) = \boldsymbol{U}\tilde{\boldsymbol{W}}_1 - \tilde{\boldsymbol{N}}^i\tilde{\boldsymbol{W}}_2, \tag{47}$$

into Equation (45) proves the theorem. □

Note that Theorem 1 is devoted to a particular battery system of Equations (15) and (16). However, it can be generalized to any system, which can be written in the form of Equations (15) and (16). Consequently, the offline design procedure reduces to:

Step 0: Solve Equation (19) to acquire $\mathcal{T}_1$ and $\mathcal{T}_2$.
Step 1: Solve Equation (39) with setting α, $0 < \alpha < 1$ to achieve $\tilde{N}^i$,U.
Step 2: Calculate:

$$K^i = U^{-1}\tilde{N}^i, \tag{48}$$

$$H^i = \mathcal{T}_1\tilde{A}^i - K^i\bar{C}, \tag{49}$$

$$M^i = \mathcal{T}_1\bar{B}^i, \tag{50}$$

$$F^i = K^i + H^i\mathcal{T}_2. \tag{51}$$

Whilst the online application procedure boils down to:

Step 0: Set the internal state of the observer initial conditions z_0, while $k = 0$.
Step 1: Determinate z_{k+1} and $\hat{x}_k$ based on Equations (17) and (18).
Step 2: Set $k = k + 1$ and move to *Step 1*.

4. Illustrative Example

This section proposes a pulsed discharge example of the battery system to validate the correctness and performance of the proposed observer. Firstly, the state vector is defined as:

$$x = \begin{bmatrix} U_1 & U_2 & SOC \end{bmatrix}^T, \tag{52}$$

where $T_s = 1$ as well as the input vector I_b is the pulsed discharge current, which operates in range $(-1, 0)$ A and has been illustrated in Figure 3a. The distribution matrices of exogenous disturbance vectors for the process and measurement uncertainties are defined as follow:

$$W_1 = 1 \cdot 10^{-6} I, \qquad W_2 = 1 \cdot 10^{-2} I. \tag{53}$$

Moreover, let us consider the following fault scenarios to validate the accuracy of the proposed observer:

$$f_{a,k} = \begin{cases} -0.3 \cdot I_{b,k} & 3000 \leq k \leq 6500 \\ 0.3 \cdot I_{b,k} & 8000 \leq k \leq 11000 \\ 0 & \text{otherwise,} \end{cases} \tag{54}$$

$$f_{s,k} = \begin{cases} y_k - 0.4 & 4500 \leq k \leq 9500 \\ 0 & \text{otherwise,} \end{cases} \tag{55}$$

along with the current and voltage measurement fault distribution matrices:

$$B_f = \frac{1}{M_m}\sum_{i=1}^{M_m} B_f^i = \begin{bmatrix} 1.856086 \\ 0.4853711 \\ 0.1389095 \end{bmatrix} \cdot 10^{-3}, \qquad C_f = \begin{bmatrix} 0 \\ 1 \end{bmatrix}. \tag{56}$$

Note that the voltage fault distribution matrix is composed of either zeros or ones. One means that the fault affects a given measurement while zero means a contradictory situation. Moreover, the disturbance distribution matrices are obtained using the experimental data and the general approach proposed in [34]. Accordingly, the voltage measurement fault $f_{s,k}$ corresponds to the possible significant measurement inaccuracies. Similarly, the current measurement fault $f_{a,k}$ corresponds to the significant loss of battery performance related to its current-based behavior. It can be clearly viewed that the voltage measurement fault distribution matrix is acquired from the system matrix C (Equation (4)) and the fault $f_{s,k}$ occurred in the state U_2. It can be easily seen that, based on Equations (54) and (55), the voltage and current measurement faults occurred, simultaneously.

Consequently, a response of the T-S fuzzy system was compared with experimental data of the Li-ion 18650 battery from the NASA benchmark [35]. The comparison has been made for battery voltage and was illustrated in Figure 3b, where the blue dash-dotted line indicates the T-S fuzzy system response along with the experimental data depicted by a black dashed line. It can be easily seen that the response of the T-S fuzzy system is very close to the experimental data.

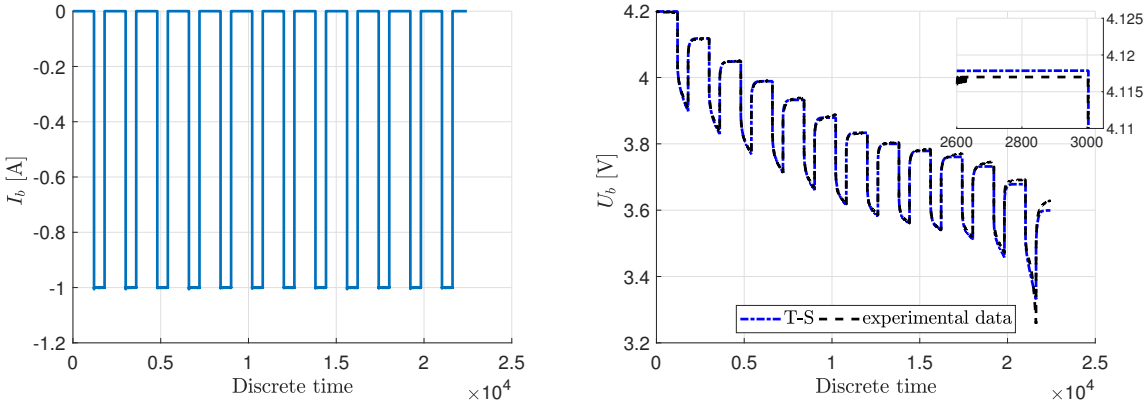

(**a**) (**b**)

Figure 3. Input vector (**a**) and comparison between experimental data and the T-S system for the battery voltage U_b (**b**).

Figure 4a,b illustrate the terminal voltage U_1 and U_2 of the first and second RC network, respectively. The state's response is given by blue dash-dotted lines, while their estimates are presented with red dashed lines as well as measured outputs indicated as light green solid lines. Figure 5a presents the battery state of charge with a blue dash-dotted line as well as its estimate depicted with a red dashed line. As can be observed, the states are properly estimated under the voltage and current measurement faults as well as the measurement uncertainties. Consequently, battery voltage U_b has been estimated with very good accuracy as presented in Figure 4b, where the state is indicated by a blue dash-dotted line along with its estimate given with a red dashed line. Moreover, Figures 6a and 7b illustrate an evolution of the state estimation error for the U_1, U_2, SOC as well as the battery voltage U_b.

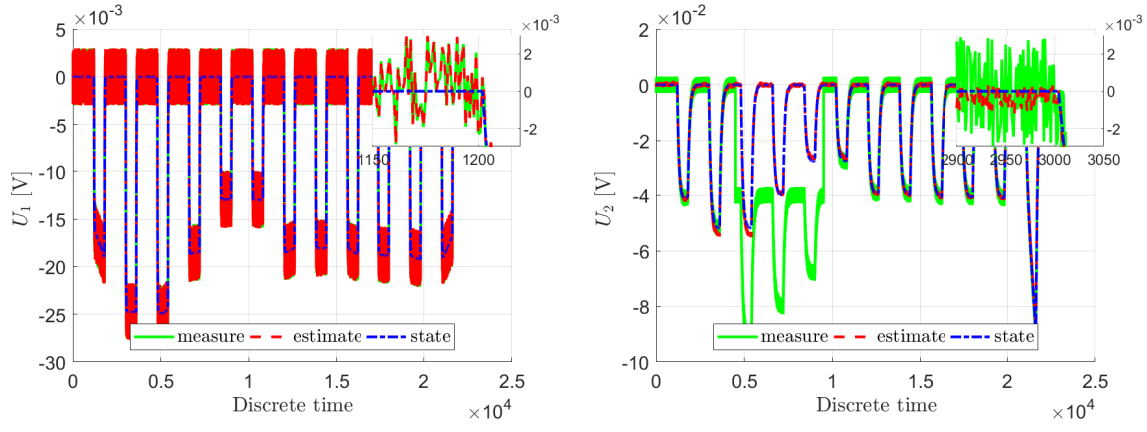

(**a**) (**b**)

Figure 4. State variables U_1 (**a**) and U_2 (**b**).

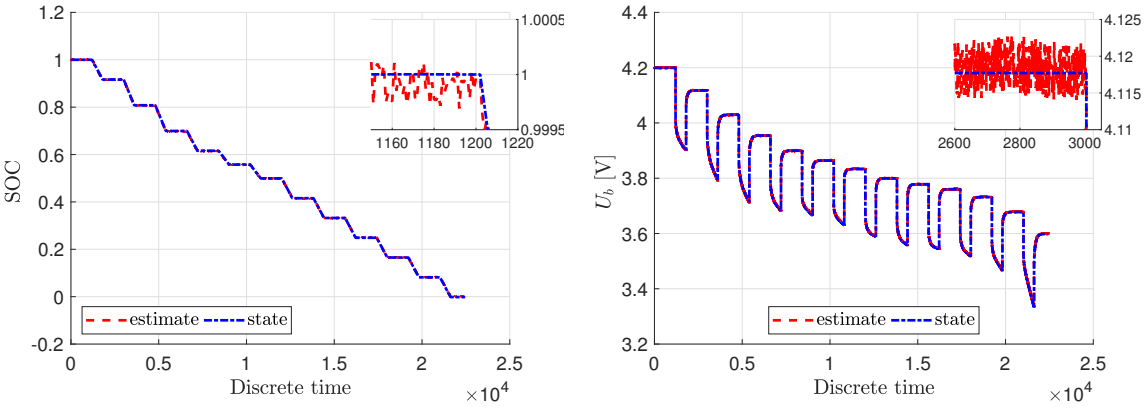

(**a**) (**b**)

Figure 5. State variable U_{soc} (**a**) and battery voltage U_b (**b**).

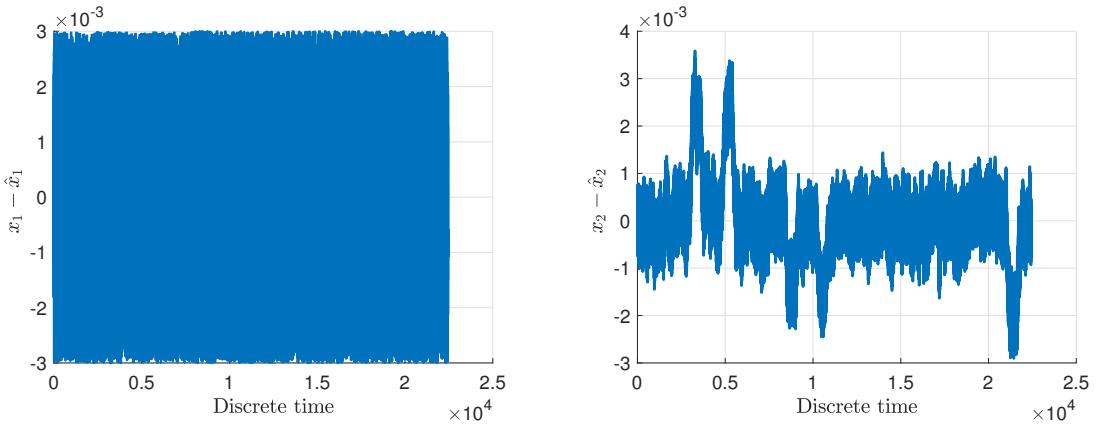

(**a**) (**b**)

Figure 6. Evolution of the state estimation error for the U_1 (**a**) and U_2 (**b**).

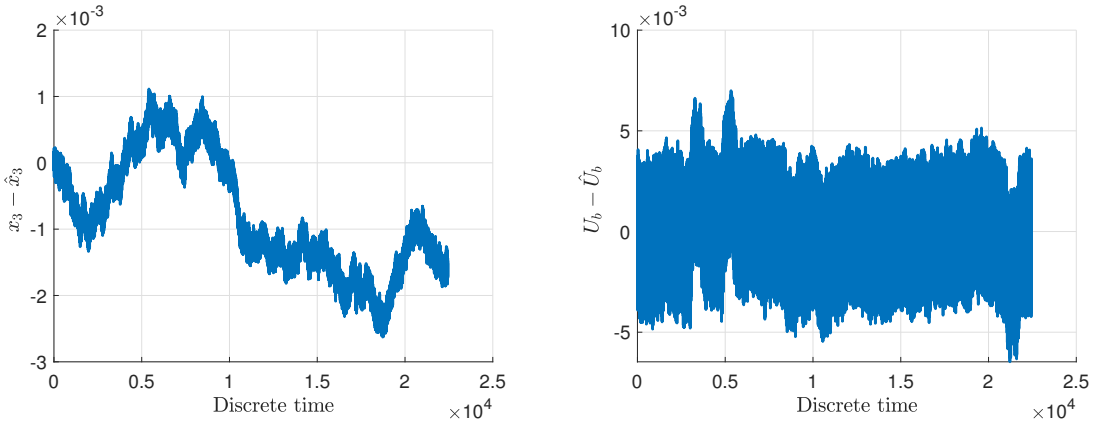

(**a**) (**b**)

Figure 7. Evolution of the state estimation error for the *SOC* (**a**) and U_b (**b**).

Additionally, a slowly developing fault is introduced and illustrated with Figure 8.

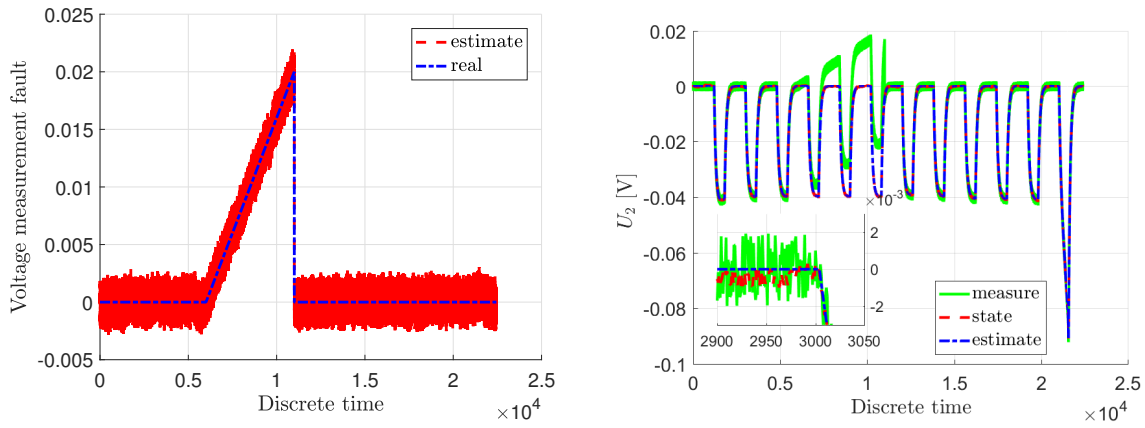

(**a**) (**b**)

Figure 8. Slowly developing voltage measurement fault (**a**) and the response of the faulty system (**b**).

Moreover, these results can be compared with another scheme based on the same NASA benchmark, for example, a Lyapunov-based observer [36]. Weit et al. described the observer for the SOC estimation along with the similar pulsed discharge current. However, these authors have assumed that the system is not occupied by any faults. The estimation Root Mean Square Errors (RMSEs) for the Lyapunov-based observer were compared with the estimation RMSEs for the proposed observer in Table 2. It can be easily seen that the novel observer has a better accuracy under the exogenous disturbances describing the process and measurement uncertainties. Additionally, the system has been occupied by the current and voltage measurement faults, simultaneously. Finally, these results confirm the performance and correctness of the proposed RUL estimation scheme for the battery system.

Table 2. The estimation errors (RMSEs) comparison between the proposed novel observer and the Lyapunov-based observer [36].

	Proposed Novel Observer	**Lyapunov-Based Observer**
U_b (mV)	2.4	5.2
U_{SOC} (mV)	0.319	26.8
SOC (%)	0.058	4.6

Furthermore, the proposed observer can form the base for RUL estimation. For that purpose a battery feeding Automated Guided Vehicles (AGVs) is considered. Indeed, the SOC for the AGV is modeled as

$$SOC_k = p_{1,k}t + p_{2,k}, \tag{57}$$

where $t = kT_s$ and $\boldsymbol{p}_k = [p_{1,k} \quad p_{2,k}]^T$ is the parameter vector relating the time t with SOC. Indeed, their values are strictly correlated with the AGV electronic equipment and DC motors fed by the batteries.

Note that the model Equation (57) can be used to predict RUL $\bar{t}$ of the batteries. It is defined as the time from SOC_k to the minimum SOC, $S\bar{O}C$. This one can be written as

$$S\bar{O}C = p_{1,k}\bar{t} + p_{2,k}. \tag{58}$$

This forms a prediction equation under current k, which leads to

$$\bar{t} = \frac{S\bar{O}C - p_{2,k}}{p_{1,k}}. \tag{59}$$

Note that the parameters $p_{1,k}$ and $p_{1,k}$ can be obtained with any recursive parameter estimation technique [37]. In this paper, the celebrated Recursive Least Squares (RLS) [38] algorithm is used. Hence, Equation (57) can be written in an alternative form

$$SOC_k = \boldsymbol{r}_k^T \boldsymbol{R}_k, \tag{60}$$

where $\boldsymbol{r}_k = [\boldsymbol{t} \quad 1]^T$.

Thus, the RLS algorithm can be formulated as follows:

Step 0: Set covariance matrix $\boldsymbol{R}_0 = \sigma \boldsymbol{I}$, where $\sigma > 0$ is a sufficiently large positive contort. Moreover, set initial parameter vector $\boldsymbol{p}_0$ and $k = 1$.

Step 1: Calculate:

$$\boldsymbol{K}_k = \frac{\boldsymbol{R}_{k-1}\boldsymbol{r}_k}{1 + \boldsymbol{r}_k^T \boldsymbol{R}_{k-1}\boldsymbol{r}_k}, \tag{61}$$

$$\boldsymbol{R}_k = \left(\boldsymbol{I} - \boldsymbol{K}_k \boldsymbol{r}_k^T\right) \boldsymbol{R}_{k-1}. \tag{62}$$

Step 2: Update parameter vector

$$\hat{\boldsymbol{p}}_k = \hat{\boldsymbol{p}}_{k-1} + \boldsymbol{K}_k \left(SOC_k - \hat{\boldsymbol{r}}_k^T \boldsymbol{p}_{k-1}\right) \tag{63}$$

Set $k = k + 1$ and move to *Step 1*.

Finally, the critical SOC is selected as $S\bar{O}C = 0.1$, which pertains to 10% of SOC. Hence, the proposed algorithm was used to estimate the remaining use of the AGV presented in Figure 9a. Moreover, Figure 9b presents the SOC denoted by Equation (57) and its critical SOC given by Equation (58). The AGV was employed to deal with a specific task and it was considered that the AGV starts with a 90% SOC. Additionally, the AGV has repeated this task until its battery has discharged until 10%. Furthermore, the estimated parameters $p_{1,k}$ and $p_{2,k}$ of the Equation (57) are presented in Figure 10a,b, respectively. Consequently, it was estimated that the AGV will deal with the task for 3013.7 seconds as it is illustrated in Figure 11.

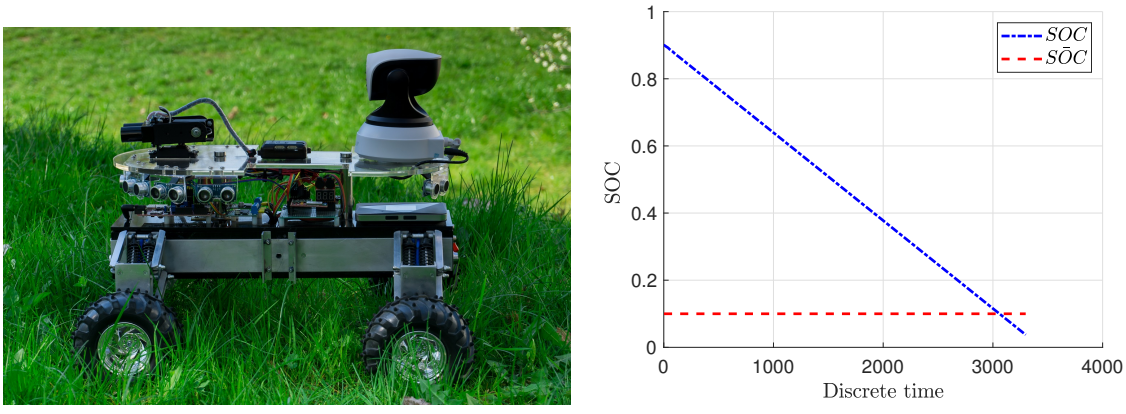

(**a**) (**b**)

Figure 9. Automated Guided Vehicle (**a**) and its State of Charge (**b**).

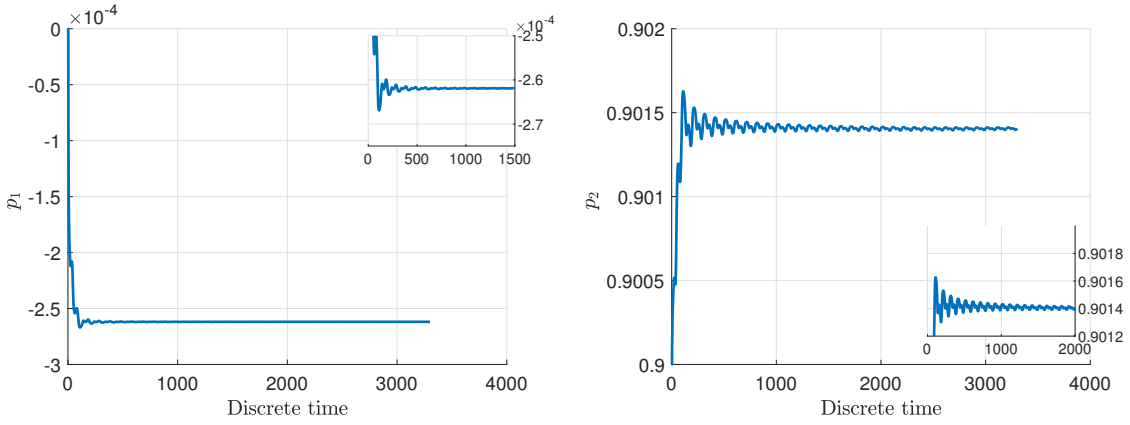

(**a**) (**b**)

Figure 10. Parameter variables p_1 (**a**) and p_2 (**b**).

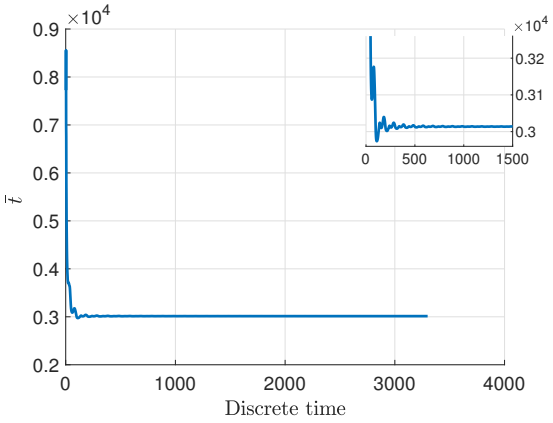

Figure 11. Time of the AGV remaining use.

5. Concluding Remarks

The paper dealt with the problem of the battery remaining useful life estimation under voltage and current measurement faults. The considered system was transformed into Takagi–Sugeno form, where the state super-vector includes the states as well as current and voltage measurement faults. External disturbances were bounded by an ellipsoid based on a so-called Quadratic Boundedness approach, which guarantees the system stability. Moreover, the Takagi–Sugeno fuzzy battery system based on a second-order RC model was considered. The proposed system is a parameter-varying one due to the fact that the parameters of the second-order RC model depend on the battery state of charge. Additionally, the response of the proposed Takagi–Sugeno fuzzy battery system was compared with the Li-ion 18650 battery experimental data. Finally, the results have confirmed the performance and accuracy of the proposed remaining useful life estimation scheme. The system states have been correctly reconstructed even in the case of simultaneous voltage and current measurement faults. Consequently, the battery voltage has been properly estimated. Moreover, the results were compared with the other scheme based on the same experimental data, which confirmed the accuracy of the proposed novel observer. In future work, the proposed scheme will be the base for the remaining useful life fault-tolerant control for a Takagi–Sugeno fuzzy system.

Author Contributions: N.K. developed entire remaining useful life estimation strategy as well as contributed to the experiments and described the experimental results. M.P. derived the design procedure for fault estimation. M.W. contributed to the development of the convergence conditions and review of the literature. All authors have read and agreed to the published version of the manuscript.

Funding: The work was supported by the National Science Centre, Poland, under Grant: UMO-2017/27/B/ST7/00620.

Conflicts of Interest: The authors declare no conflict of interest.

Appendix A

$$\boldsymbol{A}^1 = \begin{bmatrix} 0.9006406 & 0 & 0 \\ 0 & 0.9897348 & 0 \\ 0 & 0 & 1 \end{bmatrix}, \quad \boldsymbol{A}^2 = \begin{bmatrix} 0.9006746 & 0 & 0 \\ 0 & 0.9897346 & 0 \\ 0 & 0 & 1 \end{bmatrix}, \tag{A1}$$

$$\boldsymbol{A}^3 = \begin{bmatrix} 0.9006746 & 0 & 0 \\ 0 & 0.9897346 & 0 \\ 0 & 0 & 1 \end{bmatrix}, \quad \boldsymbol{A}^4 = \begin{bmatrix} 0.9010958 & 0 & 0 \\ 0 & 0.9897277 & 0 \\ 0 & 0 & 1 \end{bmatrix}, \tag{A2}$$

$$\boldsymbol{A}^5 = \begin{bmatrix} 0.8956012 & 0 & 0 \\ 0 & 0.9891699 & 0 \\ 0 & 0 & 1 \end{bmatrix}, \quad \boldsymbol{A}^6 = \begin{bmatrix} 0.8971199 & 0 & 0 \\ 0 & 0.9888847 & 0 \\ 0 & 0 & 1 \end{bmatrix}, \tag{A3}$$

$$\boldsymbol{A}^7 = \begin{bmatrix} 0.8977275 & 0 & 0 \\ 0 & 0.9885887 & 0 \\ 0 & 0 & 1 \end{bmatrix}, \quad \boldsymbol{A}^8 = \begin{bmatrix} 0.8988283 & 0 & 0 \\ 0 & 0.9884339 & 0 \\ 0 & 0 & 1 \end{bmatrix}, \tag{A4}$$

$$\boldsymbol{A}^9 = \begin{bmatrix} 0.8974476 & 0 & 0 \\ 0 & 0.9887685 & 0 \\ 0 & 0 & 1 \end{bmatrix}, \quad \boldsymbol{A}^{10} = \begin{bmatrix} 0.8963523 & 0 & 0 \\ 0 & 0.9893128 & 0 \\ 0 & 0 & 1 \end{bmatrix}, \tag{A5}$$

$$\boldsymbol{A}^{11} = \begin{bmatrix} 0.8982049 & 0 & 0 \\ 0 & 0.9890503 & 0 \\ 0 & 0 & 1 \end{bmatrix}, \quad \boldsymbol{A}^{12} = \begin{bmatrix} 0.8999915 & 0 & 0 \\ 0 & 0.9891698 & 0 \\ 0 & 0 & 1 \end{bmatrix}, \tag{A6}$$

$$\boldsymbol{A}^{13} = \begin{bmatrix} 0.9014272 & 0 & 0 \\ 0 & 0.9739134 & 0 \\ 0 & 0 & 1 \end{bmatrix}, \tag{A7}$$

$$\boldsymbol{B}^1 = \begin{bmatrix} 1.600604 \\ 0.4472455 \\ 0.1389095 \end{bmatrix} \cdot 10^{-3}, \quad \boldsymbol{B}^2 = \begin{bmatrix} 1.889744 \\ 0.4110915 \\ 0.1389095 \end{bmatrix} \cdot 10^{-3}, \quad \boldsymbol{B}^3 = \begin{bmatrix} 1.889744 \\ 0.4110915 \\ 0.1389095 \end{bmatrix} \cdot 10^{-3}, \tag{A8}$$

$$\boldsymbol{B}^4 = \begin{bmatrix} 1.897063 \\ 0.4103706 \\ 0.1389095 \end{bmatrix} \cdot 10^{-3}, \quad \boldsymbol{B}^5 = \begin{bmatrix} 1.932620 \\ 0.4334059 \\ 0.1389095 \end{bmatrix} \cdot 10^{-3}, \quad \boldsymbol{B}^6 = \begin{bmatrix} 1.901132 \\ 0.4440006 \\ 0.1389095 \end{bmatrix} \cdot 10^{-3}, \tag{A9}$$

$$\boldsymbol{B}^7 = \begin{bmatrix} 1.900210 \\ 0.4540602 \\ 0.1389095 \end{bmatrix} \cdot 10^{-3}, \quad \boldsymbol{B}^8 = \begin{bmatrix} 1.826928 \\ 0.4538913 \\ 0.1389095 \end{bmatrix} \cdot 10^{-3}, \quad \boldsymbol{B}^9 = \begin{bmatrix} 1.849684 \\ 0.4499863 \\ 0.1389095 \end{bmatrix} \cdot 10^{-3}, \tag{A10}$$

$$\boldsymbol{B}^{10} = \begin{bmatrix} 1.941584 \\ 0.4376601 \\ 0.1389095 \end{bmatrix} \cdot 10^{-3}, \quad \boldsymbol{B}^{11} = \begin{bmatrix} 1.918196 \\ 0.4467765 \\ 0.1389095 \end{bmatrix} \cdot 10^{-3}, \quad \boldsymbol{B}^{12} = \begin{bmatrix} 1.927376 \\ 0.4469707 \\ 0.1389095 \end{bmatrix} \cdot 10^{-3}, \tag{A11}$$

$$\boldsymbol{B}^{13} = \begin{bmatrix} 1.654240 \\ 1.054938 \\ 0.1389095 \end{bmatrix} \cdot 10^{-3}. \tag{A12}$$

References

1. Deng, Z.; Yang, L.; Cai, Y.; Deng, H. Online identification with reliability criterion and state of charge estimation based on a fuzzy adaptive extended Kalman filter for lithium-ion batteries. *Energies* **2016**, *9*, 472.
2. Cui, X.; He, Z.; Li, E.; Cheng, A.; Luo, M.; Guo, Y. State-of-charge estimation of power lithium-ion batteries based on an embedded micro control unit using a square root cubature Kalman filter at various ambient temperatures. *Int. J. Energy Res.* **2019**, *43*, 3561–3577.
3. Li, W.; Liang, L.; Liu, W.; Wu, X. State of charge estimation of lithium-ion batteries using a discrete-time nonlinear observer. *IEEE Trans. Ind. Electron.* **2017**, *64*, 8557–8565.
4. Song, Y.; Liu, D.; Yang, C.; Peng, Y. Data-driven hybrid remaining useful life estimation approach for spacecraft lithium-ion battery. *Microelectron. Reliab.* **2017**, *75*, 142–153.
5. Yuchen, S.; Datong, L.; Yandong, H.; Jinxiang, Y.; Yu, P. Satellite lithium-ion battery remaining useful life estimation with an iterative updated RVM fused with the KF algorithm. *Chin. J. Aeronaut.* **2018**, *31*, 31–40.
6. Wu, J.; Zhang, C.; Chen, Z. An online method for lithium-ion battery remaining useful life estimation using importance sampling and neural networks. *Appl. Energy* **2016**, *173*, 134–140.
7. Li, X.; Shu, X.; Shen, J.; Xiao, R.; Yan, W.; Chen, Z. An on-board remaining useful life estimation algorithm for lithium-ion batteries of electric vehicles. *Energies* **2017**, *10*, 691.
8. Qiu, X.; Wu, W.; Wang, S. Remaining useful life prediction of lithium-ion battery based on improved cuckoo search particle filter and a novel state of charge estimation method. *J. Power Sources* **2020**, *450*, 227700.
9. Liu, Z.; Sun, G.; Bu, S.; Han, J.; Tang, X.; Pecht, M. Particle learning framework for estimating the remaining useful life of lithium-ion batteries. *IEEE Trans. Instrum. Meas.* **2016**, *66*, 280–293.
10. Zhao, L.; Wang, Y.; Cheng, J. A hybrid method for remaining useful life estimation of lithium-ion battery with regeneration phenomena. *Appl. Sci.* **2019**, *9*, 1890.
11. Guha, A.; Patra, A. Online estimation of the electrochemical impedance spectrum and remaining useful life of lithium-ion batteries. *IEEE Trans. Instrum. Meas.* **2018**, *67*, 1836–1849.
12. Yang, J.; Peng, Z.; Wang, H.; Yuan, H.; Wu, L. The remaining useful life estimation of lithium-ion battery based on improved extreme learning machine algorithm. *Int. J. Electrochem. Sci.* **2018**, *13*, 4991–5004.
13. Zhang, D.; Dey, S.; Perez, H.E.; Moura, S.J. Remaining useful life estimation of lithium-ion batteries based on thermal dynamics. In Proceedings of the 2017 American Control Conference (ACC), Seattle, WA, USA, 24–26 May 2017; pp. 4042–4047.
14. Zhou, Y.; Huang, M.; Pecht, M. Remaining useful life estimation of lithium-ion cells based on k-nearest neighbor regression with differential evolution optimization. *J. Clean. Prod.* **2020**, *249*, 119409.
15. Wei, J.; Dong, G.; Chen, Z. Remaining useful life prediction and state of health diagnosis for lithium-ion batteries using particle filter and support vector regression. *IEEE Trans. Ind. Electron.* **2017**, *65*, 5634–5643.
16. Wang, X.; Hu, C.; Si, X.; Pang, Z.; Ren, Z. An adaptive remaining useful life estimation approach for newly developed system based on nonlinear degradation model. *IEEE Access* **2019**, *7*, 82162–82173.
17. Ren, L.; Zhao, L.; Hong, S.; Zhao, S.; Wang, H.; Zhang, L. Remaining useful life prediction for lithium-ion battery: A deep learning approach. *IEEE Access* **2018**, *6*, 50587–50598.
18. Ma, Y.; Chen, Y.; Zhou, X.; Chen, H. Remaining useful life prediction of lithium-ion battery based on Gauss–Hermite particle filter. *IEEE Trans. Control Syst. Technol.* **2018**, *27*, 1788–1795.
19. Rauh, A.; Butt, S.S.; Aschemann, H. Nonlinear state observers and extended Kalman filters for battery systems. *Int. J. Appl. Math. Comput. Sci.* **2013**, *23*, 539–556.
20. Seybold, L.; Witczak, M.; Majdzik, P.; Stetter, R. Towards robust predictive fault—Tolerant control for a battery assembly system. *Int. J. Appl. Math. Comput. Sci.* **2015**, *25*, 849–862.
21. Youren, W.; Xue, H.; Xing, G.; Zhitong, X.; Zewang, C. Fault-tolerant battery power supply for aircraft and its active equalization management. *Acta Aeronaut. Astronaut. Sin.* **2018**, *5*, 14.
22. Pan, W.; Chen, Q.; Zhu, M.; Tang, J.; Wang, J. A data-driven fuzzy information granulation approach for battery state of health forecasting. *J. Power Sources* **2020**, *475*, 228716.
23. Zhang, C.; Zhu, Y.; Dong, G.; Wei, J. Data-driven lithium-ion battery states estimation using neural networks and particle filtering. *Int. J. Energy Res.* **2019**, *43*, 8230–8241.
24. Guerra, T.M.; Kruszewski, A.; Lauber, J. Discrete Tagaki–Sugeno models for control: Where are we? *Annu. Rev. Control* **2009**, *33*, 37–47.

25. Witczak, M. *Fault Diagnosis and Fault-Tolerant Control Strategies for Non-Linear Systems*; Springer: Berlin/Heidelberg, Germany, 2014.
26. Meng, J.; Boukhnifer, M.; Delpha, C.; Diallo, D. Incipient short-circuit fault diagnosis of lithium-ion batteries. *J. Energy Storage* **2020**, *31*, 101658.
27. Samadi, M.F.; Saif, M. State-Space Modeling and Observer Design of Li-Ion Batteries Using Takagi—Sugeno Fuzzy System. *IEEE Trans. Control Syst. Technol.* **2016**, *25*, 301–308.
28. Meng, J.; Boukhnifer, M.; Diallo, D.; Wang, T. Short-Circuit Fault Diagnosis and State Estimation for Li-ion Battery using Weighting Function Self-Regulating Observer. In Proceedings of the 2020 Prognostics and Health Management Conference (PHM-Besançon), Besancon, France, 10–13 November 2020, pp. 15–20.
29. Rotondo, D.; Puig, V.; Nejjari, F.; Witczak, M. Automated generation and comparison of Takagi—Sugeno and polytopic quasi-LPV models. *Fuzzy Sets Syst.* **2015**, *277*, 44–64.
30. Chen, M.; Rincon-Mora, G.A. Accurate electrical battery model capable of predicting runtime and IV performance. *IEEE Trans. Energy Convers.* **2006**, *21*, 504–511.
31. De Oliveira, M.; Bernussou, J.; Geromel, J. A new discrete-time robust stability condition. *Syst. Control Lett.* **1999**, *37*, 261–265.
32. Alessandri, A.; Baglietto, M.; Battistelli, G. Design of state estimators for uncertain linear systems using quadratic boundedness. *Automatica* **2006**, *42*, 497–502.
33. Pazera, M.; Witczak, M. Towards robust simultaneous actuator and sensor fault estimation for a class of nonlinear systems: Design and comparison. *IEEE Access* **2019**, *7*, 97143–97158.
34. Mrugalski, M.; Luzar, M.; Pazera, M.; Witczak, M.; Aubrun, C. Neural network-based robust actuator fault diagnosis for a non-linear multi-tank system. *ISA Trans.* **2016**, *61*, 318–328.
35. Bole, B.; Kulkarni, C.S.; Daigle, M. *Adaptation of an Electrochemistry-Based Li-Ion Battery Model To Account for Deterioration Observed Under Randomized Use*; Technical Report; SGT, Inc.: New York, NY, USA, 2014.
36. Wei, J.; Dong, G.; Chen, Z. Lyapunov-based state of charge diagnosis and health prognosis for lithium-ion batteries. *J. Power Sources* **2018**, *397*, 352–360.
37. Bohn, C. Recursive Parameter Estimation for Nonlinear Continuous Time Systems Through Sensitivity Model Based Adaptive Filters. Ph.D. Thesis, University of Bochum, Bochum, Germany, 2000.
38. Xia, B.; Lao, Z.; Zhang, R.; Tian, Y.; Chen, G.; Sun, Z.; Wang, W.; Sun, W.; Lai, Y.; Wang, M. Online parameter identification and state of charge estimation of lithium-ion batteries based on forgetting factor recursive least squares and nonlinear Kalman filter. *Energies* **2018**, *11*, 3.